HNPS Advances in Nuclear Physics

Vol 21 (2013)

HNPS2013

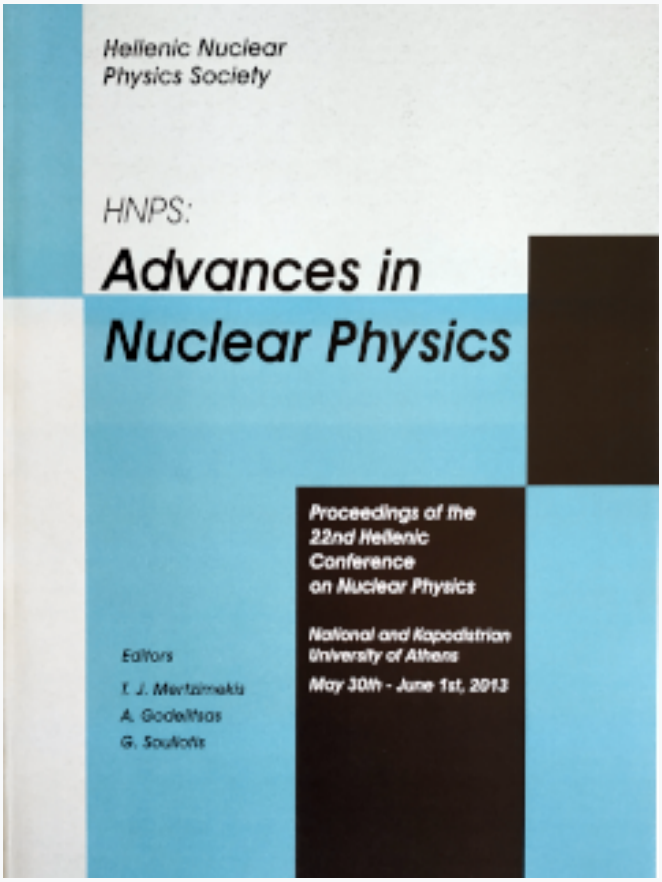

Large Sample Neutron Activation Analysis of a Peruvian Pottery Artifact

T. Vasilopoulou, I. E. Stamatelatos, E. Montoya, P. Bedregal, I. Tsalafoutas, P. Bode

doi: 10.12681/hnps.1999

Large Sample Neutron Activation Analysis of a Peruvian Pottery Artifact

T. Vasilopoulou [1a], I.E. Stamatelatos[a], E. Montoya[b], P. Bedregal[b], I. Tsalafoutas[c], P. Bode[d]

[a] *Institute of Nuclear & Radiological Sciences, Technology, Energy and Safety, National Centre for Scientific Research "Demokritos", 15310 Agia Paraskevi, Greece*
[b] *Division de Tecnicas Analiticas Nucleares, Instituto Peruano de Energia Nuclear, Av. Canada 1470, Lima 41, Peru*
[c] *Medical Physics Department, Regional Anticancer-Oncologic Hospital of Athens 'Saint Savas', Athens, Greece*
[d] *Reactor Institute Delft, Delft University of Technology, 2629JB Delft, The Netherlands*

Abstract

The present work was carried out within the first Large Sample Neutron Activation Analysis (LSNAA) intercomparison study organized under the auspices of the International Atomic Energy Agency (IAEA). Replicates of a Peruvian pottery object, representing a Pre-Columbian archaeological artifact, were prepared by the Instituto Peruano de Energia Nuclear (IPEN) and distributed to 10 laboratories with LSNAA capabilities. The LSNAA results were compared against values derived by conventional Instrumental Neutron Activation Analysis (INAA) on small amounts of the material used to produce the test object. The results of the intercomparison study will be presented in detail in a separate publication. In this work, the LSNAA methodology developed at 'Demokritos' for analysis of large and irregular shaped objects is discussed. An accurate description of the complex geometry of the object was obtained by Computerized Tomography X-ray scanning. The correction factors required for the effects of neutron self-shielding and gamma-ray self-attenuation within the large sample material were derived by Monte Carlo simulations using MCNP code. The results of the study showed that LSNAA provides elemental concentration values with a satisfactory agreement against values obtained by conventional INAA. Therefore, LSNAA is a technique suitable for the purpose of analysis of intact pottery objects of irregular shape for archaeological studies.

Keywords: Neutron Activation Analysis, Large Sample, Pottery artifact

1. Introduction

Large Sample Neutron Activation Analysis (LSNAA) is a novel technique, which enables non-destructive analysis of intact bulk objects, up to several liters in volume. In LSNAA the sample is irradiated at a research reactor graphite thermal neutron column and is subsequently transferred to a gamma ray spectrometry system to be counted either as a whole [1] or using a scanning geometry counting configuration [2]. Corrections are required for self-shielding of the activating neutrons [3, 4], self-absorption of gamma rays [5], heterogeneity of the sample [6, 7] and geometric factor during gamma counting [8]. Analysis of the acquired gamma spectra allows the evaluation of the elemental composition of the sample. Absolute [9], comparative [10], K_0 [11] and internal mono-standard [12] based calibration techniques for LSNAA have been presented.

LSNAA has been successfully applied for the analysis of large and non-standard geometry archaeological samples [13] as well as of an intact Greek ceramic vase [9]. Moreover, it was used for compositional studies on ancient pottery samples obtained from Buddhist sites of Andhra Pradesh in India [14] and authenticity identification of intact ancient Chinese porcelain ware [15].

The first LSNAA Intercomparison exercise was organized under the auspices of the International Atomic Energy Agency (IAEA) through the Coordinated Research Project (CRP) "Application of Large Sample

[1]Corresponding author at: Institute of Nuclear & Radiological Sciences, Technology, Energy and Safety, National Centre for Scientific Research "Demokritos", 15310 Agia Paraskevi, Greece, tel: +30 210 6503713, fax: +30 210 6545496, e-mail:dora@ipta.demokritos.gr

Neutron Activation Analysis for Inhomogeneous Bulk Archaeological Samples and Bulk Objects" (2010-2012). Replicates of a Peruvian pottery object, representing a Pre-Columbian archaeological artifact of the Mochica culture, were prepared by the Instituto Peruano de Energia Nuclear (IPEN) and distributed to 10 laboratories with LSNAA capabilities. Each laboratory used its methodology to analyze the bulk sample and produce quantitative results. The LSNAA results were compared against values derived by conventional Instrumental Neutron Activation Analysis (INAA) on small amounts of the material used to produce the test object. The content and the final results of this exercise will be presented in detail in a separate publication [16].

In this work, the LSNAA methodology developed at "Demokritos" for analysis of large and irregular shaped objects is discussed. An accurate description of the complex geometry of the object was obtained by Computerized Tomography X-ray scanning. The correction factors required for the effects of neutron self-shielding and gamma-ray self-attenuation within the large sample material were derived by Monte Carlo simulations using MCNP code. The results of this study revealed the capabilities of LSNAA technique for analysis of large samples and bulk objects of irregular shapes, providing an important analytical tool for non-invasive multi-elemental analysis of large samples that are too precious to remove small parts from, such as archaeological objects and artifacts.

2. Experimental

Sample

The sample analyzed was a Peruvian pottery object, representing a Pre-Columbian archaeological artifact of the Mochica culture [17]. It was an animal-shaped ceramic bottle of $25.70\,cm$ in height and $9.60\,cm$ in maximum diameter. The average wall thickness was $0.70\,cm$ and its mass was $780\,gr$. The bottle was prepared by IPEN, Peru, and shipped to the participating laboratories.

Neutron irradiation

The experimental procedures were performed at the facilities of Reactor Institute Delft, Delft University of Technology (The Netherlands). Neutron irradiation was performed at the Big Sample Neutron Irradiation System (BISNIS) installed at Hoger Onderwijs Reactor graphite thermal neutron column [18]. BISNIS provides a moderated neutron flux of $5 \times 10^8\,cm^{-2}\,s^{-1}$. The irradiation time was $48\,h$. During irradiation zinc flux monitors were positioned on the surface of the large sample.

Gamma-ray counting

A Ge detector based spectrometry system was employed for the measurement of emitted gamma rays. The detector consisted of a Ge crystal of 96% relative efficiency, $1.82\,keV$ energy resolution at the $1332\,keV$ ^{60}Co photo-peak and peak to Compton ratio of 97:1. More details for the gamma ray detection system can be found elsewhere [19]. Activation gamma ray spectra were measured 5, 6, 10 and 24 days after irradiation. During measurement the bulk sample was rotated around its vertical axis to minimize axial non-uniformity of activation. The distance from the detector surface to the axis of rotation was $20\,cm$. The acquired activation spectra were corrected with the corresponding gamma ray background spectra. Spectrum analysis was performed using Gamma Vision^{TM} software.

3. Monte Carlo simulations

The irradiation and gamma-spectrometry facilities as well as the sample were simulated using Monte Carlo code MCNP, version 5 [20]. Cross section data from the Evaluated Nuclear Data File (ENDF) system were used for the computations [21]. Since both neutron and gamma ray self-shielding factors are sample dependent, a close approximation of the studied animal-shaped bottle was required. For this purpose, Computerized Tomography (CT) X-ray Scanning was employed. The sample was scanned in vertical steps of $0.3\,cm$ using an Aquilion Toshiba 64 series CT medical system. In total 100 cross sections were acquired. In Figure 1, three cross-section views of the sample are shown, as examples. The tomography data obtained

allowed an accurate 3-D representation of the sample in the MCNP input files. A picture of the analyzed item, the corresponding MCNP sample geometry model and a CT reconstruction of the sample are shown in Figure 2.

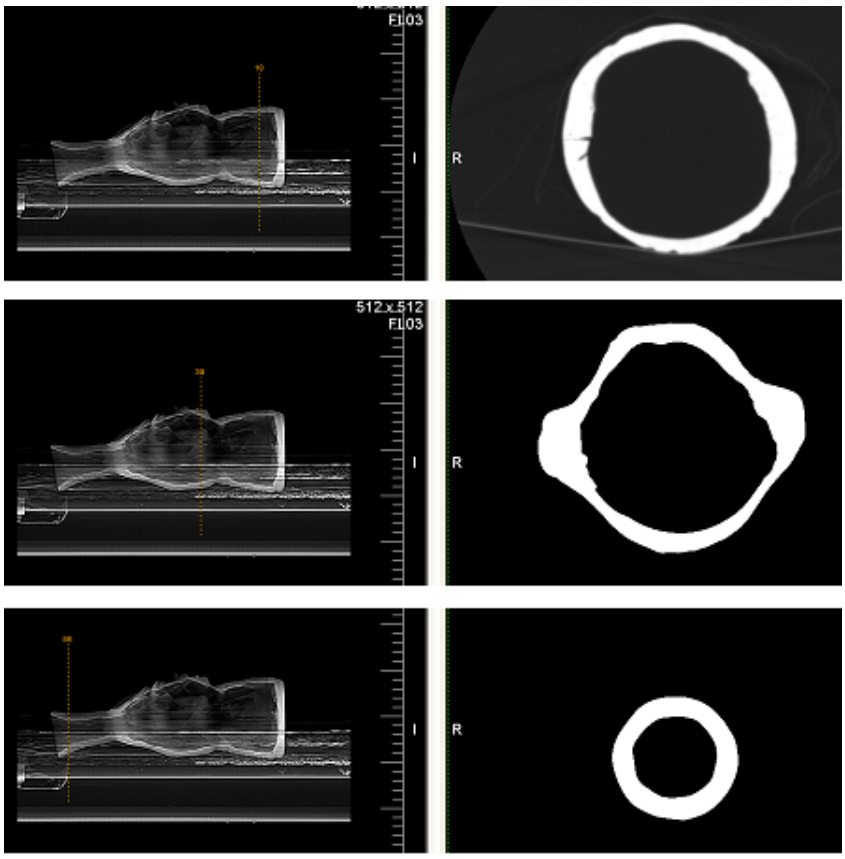

Figure 1: CT based simulation of a Peruvian Ceramic bottle (cross sectional view at three levels)

Simulations were performed assuming thermal neutrons incident on the surface of the BISNIS graphite pile. Thermal fluxes were predicted using track length estimates of neutron flux, in units of cm^{-2} per source neutron. The neutron self-shielding correction factor, f_n, was calculated as the ratio of the average predicted thermal neutron flux throughout the volume of the ceramic sample to the average predicted thermal neutron flux over its external surface. The activating neutron flux was derived by combining the experimentally determined thermal neutron flux on the surface of the sample as measured by zinc monitors and the MCNP predicted neutron self-shielding correction factor. The Ge detector Full Energy Peak Efficiency (FEPE) for the voluminous source geometry configuration was calculated using the efficiency transfer method on the basis of the FEPE measured for a reference point source [22]. MCNP code was used to predict FEPE for the reference point source at 20 cm distance from the detector (at the geometrical centre of the ceramic sample) and for the actual ceramic volume source configuration in order to derive the efficiency transfer factor for the bulk sample. Pulse height tally was used to predict the detector's response in terms of energy deposited in the active volume of the crystal in the specified energy bin and thus estimate the absolute FEPE of the detector.

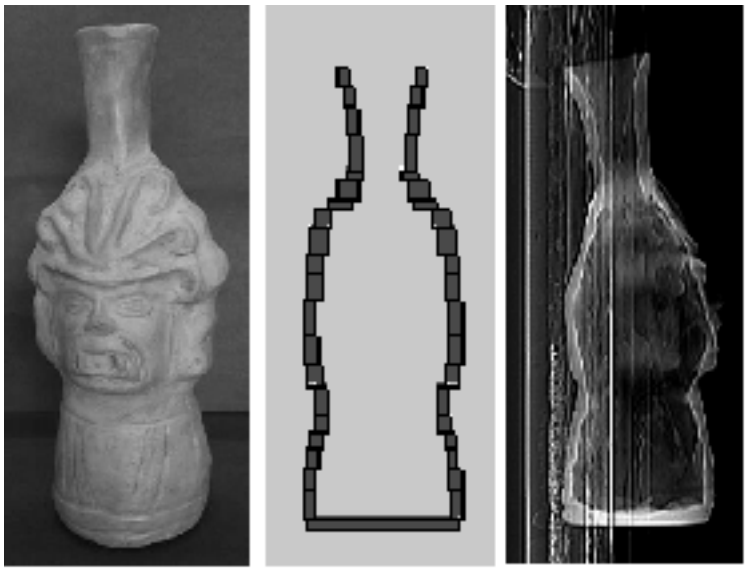

Figure 2: Picture, the corresponding MCNP sample geometry model and CT scan image of the Peruvian animal-shaped bottle (planar view)

4. Results and Discussion

Correction factors

The average thermal neutron fluence rate at the surface of the sample was $(3.91 \pm 0.33) \times 10^8\, cm^{-2}\, s^{-1}$, as measured by the zinc monitors. The MCNP predicted neutron self-shielding factor, f_n, was 0.96 ± 0.01. By applying this factor on the average thermal neutron fluence rate over the surface of the sample, the average activating neutron fluence rate within its volume was $(3.73 \pm 0.33) \times 10^8\, cm^{-2}\, s^{-1}$.

The MCNP calculated FEPE curves for the point and the actual volume source over the photon energy range from 100 to $1600\, keV$ are shown in Figure 3. The corresponding efficiency transfer function (f_γ), from point to volume source geometry, defined as the ratio of FEPE for the volume source to FEPE for the reference point source, is also plotted in this Figure. As it can be observed, for the ceramic sample studied, f_γ increases with energy. This result is explained by the decrease in photon attenuation within the ceramic material with increasing photon energy for the photon energy range studied.

The correction factors depend on material, size and shape of the large sample itself and are facility specific. Comparison of the derived correction factors for neutrons and photons showed that, for the ceramic sample examined in this study, gamma correction was the significant one. Moreover, this effect was more pronounced at lower photon energies. For example, the f_γ correction factor over the photon energy region from 100 to $1600 keV$ ranged from 0.61 to 0.78 while the neutron self-shielding correction factor f_n was 0.96. This result is in agreement with the findings of other studies showing that gamma correction was the dominant one in LSNAA [5–7].

Elemental analysis

Table 1 shows the elemental concentration results derived by LSNAA, the values obtained by conventional INAA and their ratios along with their standard uncertainties. It is noted that the reported combined uncertainties include all identified contributing sources related to nuclear data, experimental procedure and simulations. These include uncertainties in cross section data, measured neutron fluence rate, gamma ray counting and Monte Carlo computations.

To further compare the results, zeta-score per element was calculated as the difference between the LSNAA and the reference value, divided by the square root of the squares of the combined uncertainties

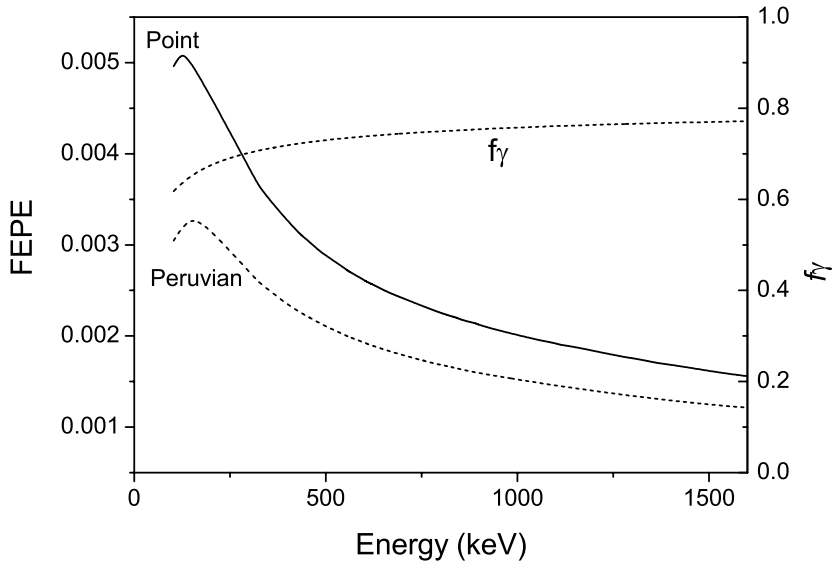

Figure 3: Predicted FEPE for the point and volume source and the calculated efficiency transfer factor (f_γ) as a function of photon energy for the ceramic sample studied

of the two. Zeta-score values are then compared to determined classification being $|z| \leq 2$ evaluated as satisfactory, $2 < |z| \leq 3$ considered of questionable quality and $|z| > 3$ considered unsatisfactory.

As it can be seen, all concentration ratios - except for Yb and Sm - are within 0.8 to 1.1, indicating a satisfactory agreement between the activation analysis results. Moreover, for almost all elements, zeta-scores range from 0.1 to 3.0. The only exception is Sm ($zeta = 6.5$). The discrepancy for Sm could be attributed to the high background signal at the lower photon energy region, which causes difficulties in the photopeak analysis. Moreover, it could be taken to suggest that the MCNP predicted FEPE curve may be inadequate at the specific energy region [9]. Therefore, for the analysis of elements emitting photons in this energy region (i.e. Sm photopeak at $103.2keV$) further optimization of the Ge detector model is required on the basis of best agreement between calculated and experimental FEPE values.

Element	LSNAA concentration (mg/kg)	INAA concentration (mg/kg)	LSNAA/INAA ratio	Zeta-score
La	19.6 ± 1.0	24.8 ± 2.1	0.8 ± 0.1	2.3
K	17240 ± 1104	16637 ± 1481	1.0 ± 0.1	0.3
Co	15.1 ± 0.9	14.8 ± 0.4	1.0 ± 0.1	0.3
Fe	36680 ± 2494	44547 ± 891	0.8 ± 0.1	3.0
Sc	16.6 ± 0.9	16.5 ± 0.8	1.0 ± 0.1	0.1
Cs	11.6 ± 1.4	11.4 ± 0.3	1.0 ± 0.1	0.2
As	31.3 ± 3.9	33.9 ± 2.2	0.9 ± 0.1	0.6
Sb	4.3 ± 0.3	5.1 ± 0.5	0.8 ± 0.1	1.4
Yb	3.3 ± 0.5	2.3 ± 0.1	1.4 ± 0.2	2.0
Cr	27.3 ± 4.0	25.1 ± 1.9	1.1 ± 0.2	0.5
Sm	3.5 ± 0.2	5.8 ± 0.3	0.6 ± 0.1	6.5

Table 1: LSNAA and INAA elemental concentrations, their ratio and zeta-scores for the pottery sample studied

5. Conclusions

LSNAA was used for the analysis of a ceramic object, representing a Pre-Columbian archaeological artifact of the Mochica culture. The required corrections for thermal neutron self-shielding during sample irradiation and γ-ray detection efficiency for the volume source during counting were derived using the Monte Carlo method enabling precise simulation of the large sample, irradiation facility and gamma ray detector configurations. A detailed representation of the complex sample geometry was performed using a 3-D CT scan of the object. A satisfactory ratio agreement within $0.8 - 1.1$ was observed for all elements, except for Yb and Sm, when LSNAA results were compared against elemental values derived by INAA.

The results of this work showed that LSNAA is a technique suitable for analysis of intact pottery objects of irregular shape and therefore contribute to the requirement for developing validated nuclear analytical procedures for non-destructive, multi-element bulk sample analysis of precious artifacts and archaeological objects that need to be preserved intact and cannot be damaged for sampling purposes. The ability to analyze whole objects distinguishes LSNAA among the analytical techniques since other established non-destructive methods (such as X-ray fluorescence analysis or analytical techniques based on charged particle irradiation-PIXE) can only analyze superficial layers of the sample and therefore provide limited information over the whole volume of the object.

Acknowledgements

This work was supported by the IAEA under Coordinated Research Project CRP-14565 (2010- 2012).

References

[1] R. M. W. Overwater, P. Bode, J. J. M. De Goeij, J. E. Hoogenboom, Feasibility of elemental analysis of kilogram-size samples by instrumental neutron activation analysis, Anal. Chem. 68 (1996) 341–348.

[2] M. Blaauw, H. W. Baas, M. Donze, Height-resolved large-sample INAA of a 1 m long, 13 cm diameter ditch-bottom sample, Nucl. Inst. Meth. in Phys. Research A 505 (2003) 512–516.

[3] F. Tzika, I. E. Stamatelatos, Thermal neutron self-shielding correction factors for large sample instrumental neutron activation analysis using the mcnp code, Nucl. Instr. Meth. in Phys. Research B 213 (2004) 177–181.

[4] I. H. Degenaar, M. Blaauw, J. J. M. De Goeij, Correction for neutron self-shielding in large-sample prompt-gamma neutron activation analysis, J. Radioanal. Nucl. Chem. 257 (2003) 467–470.

[5] F. Tzika, I. E. Stamatelatos, J. Kalef-Ezra, P. Bode, Large sample neutron activation analysis: Correction for neutron and gamma attenuation, NUKLEONIKA 49 (3) (2004) 115–121.

[6] R. M. W. Overwater, P. Bode, Computer simulations of the effects of inhomogeneities on the accuracy of large sample INAA, Appl. Radiat. Isot. 49 (8) (1998) 967–976.

[7] F. Tzika, I. E. Stamatelatos, J. Kalef-Ezra, Neutron activation analysis of large volume samples: The influence of inhomogeneity, J. Radioanal. Nucl. Chem. 271 (2007) 233–240.

[8] R. M. W. Overwater, P. Bode, J. J. M. De Goeij, Gamma-ray spectroscopy of voluminous sources - Corrections for source geometry and self-attenuation, Nucl. Inst. Meth. in Phys. Research A 324 (1993) 209–218.

[9] I. E. Stamatelatos, F. Tzika, T. Vasilopoulou, M. J. J. Koster-Ammerlaan, Large sample neutron activation analysis of a ceramic vase, J. Radioanal. Nucl. Chem. 283 (2010) 735–740.

[10] P. A. Beeley, R. G. Garrett, Neutron activation analysis of multiple large geological samples by in-pool irradiation using a slowpoke-2 reactor, J. Radioanal. Nucl. Chem. 167 (1) (1993) 177–185.

[11] M. Blaauw, The k0 calibration of the IRI system for INAA of samples in the kg range, J. Radioanal. Nucl. Chem. 220 (1997) 233–235.

[12] A. G. C. Nair, R. Acharya, K. Sudarshan, S. Gangotra, A. V. R. Reddy, S. B. Manohar, A. Goswami, Development of an internal monostandard instrumental neutron activation analysis method based on in situ detection efficiency for analysis of large and nonstandard geometry samples, Anal. Chem. 75 (2003) 4868–4874.

[13] K. Sueki, Y. Oura, W. Sato, H. Nakahara, T. Tomizawa, Analysis of archaeological samples by the internal monostandard method of PGAA, Journal of Radioanalytical and Nuclear Chemistry 234 (1998) 27–31.

[14] K. B. Dasari, R. Acharya, K. K. Swain, N. Lakshmana Das, A. V. R. Reddy, Analysis of large and non-standard geometry samples of ancient potteries by internal monostandard neutron activation analysis using in situ detection efficiency, J. Radioanal. Nucl. Chem. 286 (2010) 525–531.

[15] F. Songlin, F. Xiangqian, Y. Lingtong, L. Li, Methodology study of NAA techniques with neutron tube in distinguishing provenance and identifying authenticity of intact ancient ceramic ware, in: 2nd RCM of the IAEA CRP on Application of LSNAA for Inhomogeneous Bulk Archaeological Samples and Bulk objects, Delft, The Netherlands, 2010.

[16] IAEA (Ed.), Innovative Neutron Activation Analysis of Large Objects with Emphasis on Archaeology, Radiation Technology Series, IAEA, in preparation.

[17] E. Montoya, LSNAA of archaeological pottery: How to get accurate results in a practical way, in: 2nd RCM of the IAEA CRP on Application of LSNAA for Inhomogeneous Bulk Archaeological Samples and Bulk objects, Delft, The Netherlands, 2010.
[18] R. M. W. Overwater, J. E. Hoogenboom, Accounting for the thermal flux depression in voluminous samples for the instrumental neutron activation analysis, Nucl. Sci. Eng. 117 (1994) 141–157.
[19] P. Bode, R. M. W. Overwater, J. J. M. De Goeij, Large-sample neutron activation analysis: Present status and prospects, J. Radioanal. Nucl. Chem. 216 (1) (1997) 5–11.
[20] X-5 Monte Carlo Team, MCNP - A General Monte Carlo N-Particle Transport Code, Version 5, LA-UR-03-1987 (April 2003).
[21] P. F. Rose, Compiler and editor, ENDF-201, ENDF/B-VI Summary Documentation, BNL-NCS-17541, Brookhaven National Laboratory (October 1991).
[22] F. Piton, M.-C. Lepy, M.-M. Be, J. Plagnard, Efficiency transfer and coincidence summing corrections for γ-ray spectrometry, Appl. Radiat. Isot. 52 (2000) 791–795.